ingegneria sismica
International Journal of Earthquake Engineering
Anno XLIII - Num. 3 - 2026

Research on Logistics Carbon Emission Accounting Method and Emission Reduction Path Optimization in Green Supply Chain Management

Hongli Liu[1,*] *and Shuyu Sun*[1]

[1] School of Humanities and Management, Xi'an Traffic Engineering Institute, Xi'an, Shaanxi, 710300, China

SUMMARY: *In the low-carbon transition of green supply chains, only continuous technological innovation can turn challenges into opportunities. However, significant costs and externalities associated with research and development may undermine companies' willingness to invest in low-carbon R&D. This paper comprehensively considers transportation costs, transshipment costs, refrigeration costs, and carbon emissions factors to construct a green logistics carbon emissions prediction model based on the ARIMA model. It calculates the carbon emissions from railway freight transportation in the Beijing-Tianjin-Hebei region from 2004 to 2021. The results indicate that the ARIMA model has good predictive performance and can be used to predict future carbon emissions from green railway freight transportation in the Beijing-Tianjin-Hebei region. A carbon reduction path optimization model is established with the objective of minimizing the sum of fixed costs, transportation costs, refrigeration costs, carbon emissions costs, and time window penalty costs. By combining the NSGA-II algorithm with a neighborhood search algorithm, an improved NSGA-II algorithm model is designed. This algorithm is used to solve path scheduling schemes for carbon reduction path optimization model distribution and standalone path distribution under different customer scales. Experimental results show that compared to Path 1, Path 2, and Path 3, the carbon emission reduction path optimization model reduces emissions by 19.25%, 9.75%, and 7.80%, respectively. When the customer scale is large, using the carbon emission reduction path optimization model is more advantageous for cost savings.*

KEYWORDS: *carbon emissions; ARIMA model; emission reduction path; NSGA-II*

1 Introduction

As the global population continues to grow, the consumption of environmental resources is increasing, leading to the depletion of resources. The conflict between economic growth and environmental protection is increasingly attracting the attention of supply chain management scholars. In today's rapidly developing society, traditional supply chains can no longer meet the demands of the times. Faced with the issue that some companies lack the capability to deliver products that meet the needs and actual purchases of end-users, modern enterprises must strengthen green supply chains to better adapt to the development of contemporary society [1-4]. Under the backdrop of sustainable development, supply chain management that aims to minimize the environmental impact of suppliers on end-users is referred to as "green supply

*17392216060@163.com
https://doi.org/10.65102/is20261091
Published: 10 June, 2026

chain management" [5]. Compared to traditional supply chain management, green supply chain management primarily focuses on implementing green development strategies while alleviating external environmental pressures and stimulating internal innovation within enterprises [6-8].

Green supply chains encompass all logistics activities in traditional supply chains, as well as management processes such as green design, green procurement, green production, green processing, and green marketing [9, 10]. They emphasize the adoption of environmental measures at every stage of the supply chain, such as using clean energy, optimizing logistics routes, reducing packaging materials, and improving energy efficiency, to minimize negative environmental impacts [11-13]. Therefore, it is necessary to accelerate the development of modern logistics based on supply chain management. This involves establishing a scientific, systematic, and applicable method for calculating green logistics carbon emissions and optimizing pathways, and implementing comprehensive, all-encompassing green logistics management across all stages and domains [14-17]. By continuously improving the rational allocation and efficient utilization of logistics resources, we can systematically advance the transformation of logistics development within green supply chain management [18, 19].

This paper proposes a green logistics carbon emissions prediction model based on the ARIMA model, using carbon emission factors for transportation costs, transshipment costs, and refrigeration costs. First, it visually presents the carbon emissions from railway freight transportation in the Beijing-Tianjin-Hebei region from 2004 to 2024. Then, it uses the prediction model to dynamically forecast the future carbon emissions from railway freight transportation in the Beijing-Tianjin-Hebei region, completing the empirical analysis. A carbon emission reduction path optimization model is established with the objective of minimizing the sum of transportation costs, refrigeration costs, carbon emission costs, and time window penalty costs. The NSGA-II algorithm is improved using a neighborhood search algorithm to enhance its search capabilities. The improved NSGA-II algorithm is used to solve the model, ultimately yielding the total costs under different customer scales.

2 Calculation and prediction of logistics carbon emissions in green supply chain management

2.1 Carbon emissions calculation method

Cold chain logistics multimodal transport generates significant energy consumption and carbon dioxide emissions during the transportation process, transshipment at transfer nodes, and refrigeration throughout the entire process. Methods for calculating carbon emissions include life cycle assessment, IPCC calculation, input-output analysis, and total energy consumption analysis. Considering the characteristics of the research subject in this paper, we draw on the calculation methods used in relevant literature, combining the IPCC calculation method with the total energy consumption analysis method, and then collect relevant data for further study.

2.2 Carbon emissions calculation

2.2.1 Calculation of carbon emissions during transportation

Carbon emissions generated during transportation are mainly related to factors such as fuel consumption, mode of transportation, transportation distance, and freight volume. The calculation formula is as follows:

$$C_1 = \sum_{i,j \in N} \sum_{k \in K} u_k^a q_{ij}^k l_{ij}^k e_a x_{ij}^k \tag{1}$$

Among these, u_k^a denotes the unit consumption of fuel a under transportation mode k; q_{ij}^k denotes the cargo volume transported from node i to node j under transportation mode k; l_{ij}^k denotes the transportation distance from node i to node j under transportation mode k; e_α denotes the carbon emission coefficient of fuel a; x_{ij}^k takes the value 0 or 1, where $x_{ij}^k = 1$ indicates transportation from node i to node j via transportation mode k, and $x_{ij}^k = 0$ otherwise.

2.2.2 Calculation of carbon emissions during transit

Refrigerated goods can be transported by road, rail, or waterway in multimodal transport. When transferring between road-rail, road-water, and rail-water modes, certain facilities and equipment must be used to complete the transfer. This process generates a certain amount of carbon dioxide emissions, and the resulting environmental impact cannot be ignored. The formula for calculating carbon emissions generated during the transfer process is as follows:

$$C_2 = \sum_{i,j \in N} \sum_{k,l \in K} e_i^{kl} q_{ij}^k r_i^{kl} \tag{2}$$

Among these, e_i^{kl} refers to the carbon emission coefficient of the transshipment vehicle used when converting cold chain products from transportation mode k to transportation mode l at node i; r_i^{kl} takes a value of 0 or 1, where $r_i^{kl} = 0$ indicates that no change in transportation mode occurs at node i, and otherwise indicates a change in transportation mode.

2.2.3 Carbon emission calculation methods in the refrigeration process

To ensure the quality of cold chain products and reduce cargo damage, cold chain goods must be transported using special facilities and equipment to maintain the temperature at an appropriate low level. These special facilities and equipment consume energy and produce carbon dioxide while maintaining low temperatures inside the containers. The carbon emissions generated by refrigeration during the entire transportation process are calculated as follows:

$$C_3 = \sum_{i,j \in N} \sum_{k \in K} q_{ij}^k l_{ij}^k e \tag{3}$$

Among them, e refers to the amount of carbon dioxide generated per unit of transport volume and per unit of transport distance due to refrigeration.

Therefore, the total amount of carbon dioxide C generated in the multimodal transport process of cold chain logistics is:

$$C = C_1 + C_2 + C_3 \tag{4}$$

2.3 Green logistics carbon emission prediction based on the ARIMA model

2.3.1 ARIMA model

The full name of the ARIMA model is the Autoregressive Integrated Moving Average model, which was first proposed by Box and Jenkins [20]. The basic idea of the ARIMA model is to treat time-varying data sequences as random sequences and construct models to approximate their descriptions, then use past and present values of time series data to predict future values [21]. Box-Jenkins-type methods typically perform differencing on non-stationary time series for prediction, forcing them to become stationary before modeling.

An autoregressive model is a regression where the value at the current time point is equal to the value at past time points. If it depends on the past p historical values, then the order is p, denoted as $AR(p)$, and the expression is:

$$X_t = \partial_1 X_{t-1} + \partial_2 X_{t-2} + \cdots + \partial_p X_{t-p} + \varepsilon_t \tag{5}$$

where δ is the autoregressive coefficient, and ε_t is the fluctuation value in the white noise time series.

The moving average model influences the forecast value at the current time point through a linear combination of historical white noise in the time series. The principle is that historical white noise indirectly influences the predicted value at the current time point by affecting historical time series values. If a white noise sequence is $\{\varepsilon_1, \varepsilon_2, ..., \varepsilon_n\}$, then the q-order moving average model is denoted as $MA(q)$. Its expression is:

$$X_t = \mathcal{E}_t + \partial_1 \mathcal{E}_{t-l} + \partial_2 \mathcal{E}_{t-2} + \cdots + \partial_q \mathcal{E}_{t-q} \tag{6}$$

The $ARIMA$ model is based on the $ARIMA$ model, introducing the difference term d to solve the problem of non-stationarity in time series. The specific expression is:

$$\left(1 - \sum_{i=1}^{p} \varepsilon_i L^i\right)(1-L)^d X_t = \left(1 + \sum_{i=1}^{q} \varepsilon_i L^i\right)\gamma_t \tag{7}$$

The difference operator expression is:

$$\Delta^d X_t = (1-L)^d X_t \tag{8}$$

Make W_t equal to:

$$W_t = \Delta^d X_t = (1-L)^d X_t \tag{9}$$

Obtainable $ARIMA$ model variation:

$$W_t = \partial_1 W_{t-1} + \cdots + \partial_p W_{t-p} + \sigma + \varepsilon_t + \partial_1 \varepsilon_{t-1} + \cdots + \partial_q \varepsilon_{t-q} \tag{10}$$

Therefore, the three important parameters used in $ARIMA(p,d,q)$ modeling are: the number of autoregressive terms p in the AR (autoregressive model), the number of moving average terms q in the MA (moving average model), and the order of differencing d that converts a non-stationary time series into a stationary one.

2.3.2 Data Sources

The study is based on time series statistical results of carbon emissions from rail freight transportation in the Beijing-Tianjin-Hebei region from 2004 to 2024. Based on the above data, an ARIMA model was constructed to make a five-year forecast.

2.3.3 Model Construction

Using Eviews and SPSS software, we performed parameter ordering, estimation, and testing for the model. The results are shown in Tables 1 and 2. It can be seen that the data series after first-order differencing passed the unit root test at the 5% significance level. The mean values of the autocorrelation and partial autocorrelation functions are close to 0, so the parameter d = 1.

Table 1: Carbon emission ADF test results

Carbon emission	ADF test value	P value	Judging conclusion
Horizontal statistic	-2.478564	0.3843	Uneven stability
First order difference statistics	-2.385726	0.0211	smoothness **

Table 2: The first order difference sequence of carbon emissions

Year	Carbon emission /%
2004	3.31
2005	4.16
2006	12.96
2007	0.39
2008	7.30
2009	-3.50
2010	-4.24
2011	-2.24
2012	-0.77
2013	-10.51
2014	-18.38
2015	-4.02
2016	-9.79
2017	-5.07
2018	-7.16
2019	-17.02
2020	-24.78
2021	3.01
2022	3.65
2023	7.51
2024	6.57

(1) Parameter order determination and selection

Figure 1 shows the autocorrelation plot and partial autocorrelation plot of the first-order difference sequence of carbon emissions. In both plots, the functions tend to 0 after the first order and exhibit tailing phenomena. Therefore, an ARMA model should be established, where the p-value of the model is 1 and the q-value can be 0 or 1. Using Eviews software, models with different q-values were established to analyze their significance. In SPSS software, the BIC criterion is used to select the group of q values with the smaller BIC value, ultimately completing the selection of the optimal order array.

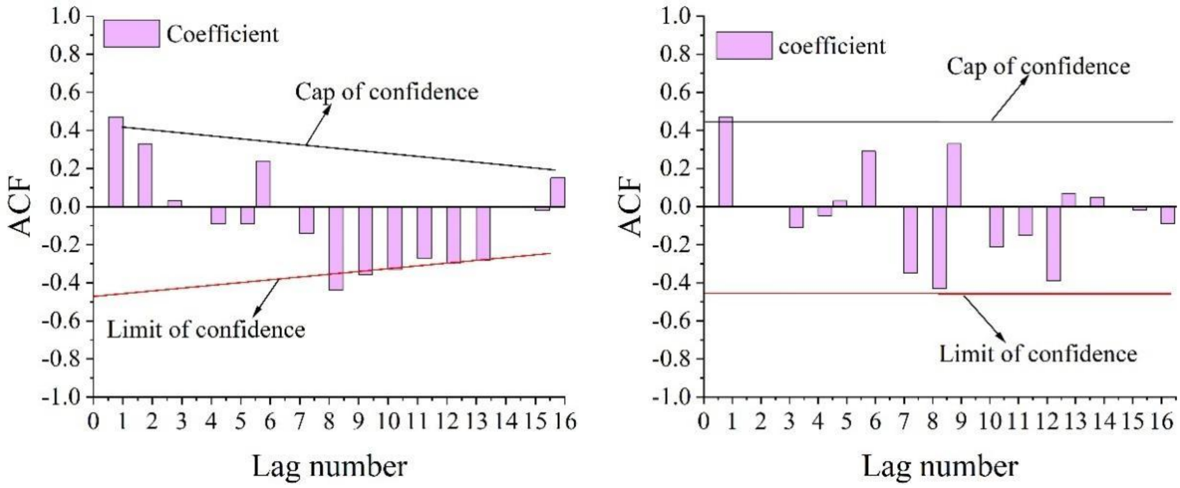

(a) Autocorrelation (b) Partial autocorrelation

Figure 1: Autocorrelation and partial autocorrelation diagrams of first-order difference sequences

The results are shown in Tables 3 and 4. Among them, all parameters of the model with order (1,1,0) are significant at the 5% level, while the MA(1) of the model with order (1,1,1) is not significant at the 5% level. The calculation results of the SPSS software show that the BIC value of the model with order (1,1,0) is smaller than that of the model with order (1,1,1), indicating that the ARIMA model with order (1,1,0) is more suitable for forecasting the time series.

Table 3: Significance of parameters in ARIMA models with different orders

(1,1,0) The significance of each parameter of ARIMA model				
Variable	Coefficient	Standard error	T statistic	P value
C	139.0321	41.12325	3.752783	0.0013
AR(1)	0.945708	0.092143	15.27531	0.0001
SIGMASQ	78.85342	26.11745	3.224722	0.0051
(1,1,1) The significance of each parameter of ARIMA model				
Variable	Coefficient	Standard error	T statistic	P value
C	140.2714	38.170437	3.891754	0.0008
AR(1)	0.931726	0.102746	12.31826	0.0001
MA(1)	0.442103	0.284132	2.773219	0.1841
SIGMASQ	61.89375	29.29745	2.157592	0.0628

Table 4: The parameters of the two prediction models are calculated

Exponent	R^2	RMSE value	BIC value	Yang-Baxter Q-statistic	Yang-Baxter P-value
(1,1,0)	0.957	7.579	5.278	17.972	0.628
(1,1,1)	0.957	7.891	5.417	17.642	0.473

(2) Residual sequence white noise test and prediction results table

The results of the residual sequence white noise test for the model are shown in Figure 2. As shown in Table 4, the Q statistic is 17.972, and the p-value is 0.628, which is significantly greater than 0.05. Additionally, all residual values of the model are within twice the standard error value, indicating that the residuals form a white noise sequence. These results suggest that the ARIMA model has good predictive performance and can be used to forecast future carbon emissions from green freight transportation in the Beijing-Tianjin-Hebei region.

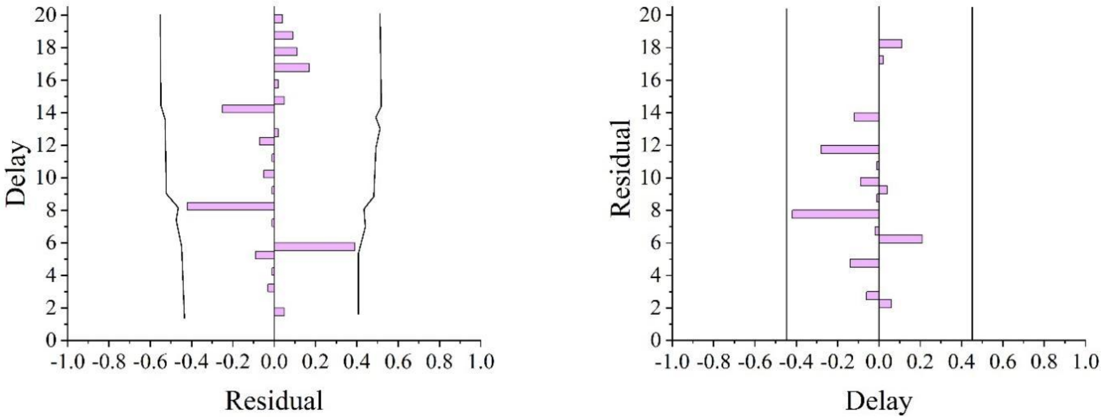

(a) Residual ACF (b) Residual PACF

Figure 2: White noise test of ARMA model

2.3.4 Case Study

The line chart comparing the ARIMA model's predicted carbon emissions with actual values is shown in Figure 3. The figure shows that the predicted values are not significantly different from the actual values, indicating that the prediction results are relatively accurate.

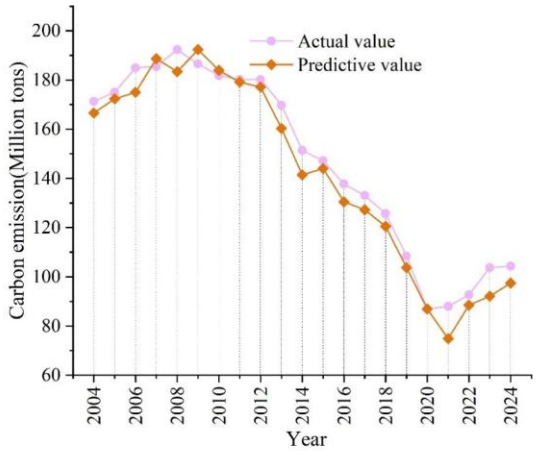

Figure 3: Comparison between simulated and actual carbon emissions of ARNMA model

3 Optimization model for carbon emission reduction in green supply chain logistics

3.1 Problem Description

The problem studied in this paper can be defined as a complete directed graph $G = (V, E)$, where the vehicle speed is constantly changing. The node set $V = V_c \cup \{0\}$ is defined, where V_c is the customer set and 0 represents the distribution center. The edge set $E = \{(i, j): i, j \in V, i \neq j\}$ is defined, and d_{ij} is the length of the arc $e(i, j)$, i.e., the distance between customers or between customers and the distribution center. $K = \{k \mid k = 1, 2, \cdots \mid K \mid\}$ is the set of homogeneous delivery vehicles, h_k denotes the set of cargo compartments of vehicle k, and Q_k^h denotes the maximum payload of cargo compartment h of vehicle k, where $h \in h_k$. P is the set of cold chain product types, $P = \{p \mid p = 1, 2, \cdots \mid P \mid\}$, $[e_i, l_i]$ is the delivery time window for customer i. If the vehicle arrives before e_i, it must wait until e_i to provide delivery services. The service duration for customer i is s_i, q_i^p is the demand quantity of customer i for product ρ, y_i^k is the departure time of the vehicle from point i, and T_m is the carbon quota. If vehicle k travels from customer i to customer j, then x_{ij}^k is 1; otherwise, it is 0. If customer i's demand for p types of cold chain goods is met by vehicle k's cargo compartment h, then y_{ip}^{kh} is 1; otherwise, it is 0.

3.2 Objective Function Design

3.2.1 Fixed Costs

Fixed costs include vehicle depreciation, maintenance, and labor costs, which can be calculated as follows:

$$FC = c_1 \sum_{k \in K} \sum_{j \in V_c} x_{oj}^k \tag{11}$$

In equation (11), FC is the fixed cost, and c_1 is the vehicle dispatch cost.

3.2.2 Transportation Costs

Transportation costs refer to the variable costs incurred by each vehicle for distribution activities, mainly including fuel consumption, maintenance, and other costs. The main influencing factors include distance, refrigeration capacity, and displacement.

$$TC = c_2 \sum_{k \in K} \sum_{i \in V} \sum_{j \in V} d_{ij} x_{ij}^k \tag{12}$$

In equation (12), TC is the transportation cost, and c_2 is the transportation cost per unit mileage traveled by the vehicle.

3.2.3 Cooling costs

Due to the perishable nature of cold chain products and the high temperature requirements during delivery, a certain amount of refrigeration costs are incurred. Refrigeration costs are divided into three parts: first, refrigeration costs during transportation; second, refrigeration costs during vehicle waiting time; and third, refrigeration costs incurred during vehicle service due to the opening and closing of the cargo compartment doors. The detailed calculation process for refrigeration costs is as follows:

$$RC = RC_1 + RC_2 + RC_3 \tag{13}$$

$$RC_1 = c_3^1 \sum_{k\in K} \sum_{i\in V} \sum_{j\in V} x_{ij}^k t_{ij} \tag{14}$$

$$RC_2 = c_3^1 \sum_{k\in K} \sum_{i\in V} \sum_{j\in V} \max((e_j - (t_i^k + s_i + t_{ij}))x_{ij}^k, 0) \tag{15}$$

$$RC_3 = c_3^2 \sum_{i\in V} s_i \tag{16}$$

In Equation (14), RC_1 represents the refrigeration cost during transportation, and in Equation (15), RC_2 represents the refrigeration cost during waiting. c_3^1 is the refrigeration cost per unit of transportation and waiting time; in Equation (16), RC_3 represents the refrigeration cost during service, and c_3^2 is the refrigeration cost per unit of service time.

3.2.4 Carbon Emission Costs

Carbon emission costs can be divided into carbon emissions generated by fuel consumption during vehicle operation and fuel consumption during vehicle refrigeration. Fuel consumption during vehicle delivery is related to the distance traveled and the delivery volume, while fuel consumption during the refrigeration process is related to time.

$$CC = CC_1 + CC_2 - c_4 T_m \tag{17}$$

$$CC_1 = c_4 \sum_{k\in K} \sum_{i\in V} \sum_{j\in V} e(F_0 + \frac{F^* - F_0}{\sum_{h\in h_k} Q_k^h} \sum_{p\in P} u_{ij}^{kp}) d_{ij} x_{ij}^k \tag{18}$$

In equation (18), CC_1 is the carbon emission cost generated by fuel combustion during the transportation process, where F_0 is the fuel consumption per unit distance when unloaded, and F^* is the fuel consumption per unit distance when fully loaded.

$$\begin{aligned} CC_2 = {} & c_4 \sum_{k\in K} \sum_{j\in V} \sum_{i\in V} e(\sum_{p\in P} u_{ij}^{k_p} E_1^p)(t_{ij} + \max(e_j - (t_i^k + s_i + t_{ij}), 0)) x_{ij}^k \\ & + c_4 \sum_{k\in K} \sum_{i\in V} \sum_{j\in V} e(\sum_{p\in P} (u_{ij}^{kp} E_2^p - \frac{q_i^p}{2}) x_{ij}^k) s_j \end{aligned} \tag{19}$$

In equation (19), CC_2 represents the carbon emission cost generated by refrigerant consumption, c_4 represents the unit carbon trading price, e represents the carbon emission coefficient, E_1^p represents the fuel consumption for refrigeration during the transportation and waiting process for product category p per unit time, and E_2^p represents the fuel consumption for refrigeration during the service process for product category p per unit time. u_i^{kp} is the weight of product category p loaded by vehicle k when passing through arc $e(i, j)$.

3.2.5 Time Window Penalty Cost

Due to the strong time sensitivity of cold chain logistics distribution, this paper introduces a penalty cost function to improve distribution service quality. Whether vehicles arrive early or late, it will reduce customer satisfaction and affect the service of remaining customers, and companies will need to pay the corresponding penalty costs.

$$\begin{aligned} TP = & \sum_{k\in K}\sum_{j\in V}\sum_{i\in V} c_5^1 x_{ij}^k \max((e_i - t_i^k), 0) \\ & + \sum_{k\in K}\sum_{j\in V}\sum_{i\in V} c_5^2 x_{ij}^k \max((t_i^k - l_i), 0) \end{aligned} \tag{20}$$

In equation (20), TP is the time window penalty cost, t_i^k is the time at which vehicle k arrives at customer i, and c_5^1 and c_5^2 are the unit penalty costs for early arrival and late arrival, respectively.

3.3 Model Establishment

Based on the above, the mixed integer programming model is established as follows:

$$\min f = FC + TC + RC + CC + TP \tag{21}$$

$$\sum_{j\in V_e} x_{0j}^k = \sum_{i\in V_e} x_{i0}^k = 1 \quad \forall k \in K \tag{22}$$

$$\sum_{i\in V} x_{ij}^k \geq y_{jf}^{kb} \quad \forall j \in V_c, k \in K, h \in h_k, p \in P \tag{23}$$

$$\sum_{i\in V}\sum_{k\in K} x_{ij}^k = \sum_{i\in V}\sum_{k\in K} x_{ji}^k \quad \forall j \in V_c \tag{24}$$

$$\sum_{i\in V_e} y_{iP}^{kb} q_i^p \leq Q_k^b \quad \forall k \in K, h \in h_K, p \in P \tag{25}$$

$$\sum_{i\in V} x_{ij}^k \leq \sum_{\rho\in P} y_{j\rho}^{kb} \quad \forall j \in V, k \in K, h \in h_k \tag{26}$$

$$t_j^k = (t_i^k + t_{ij} + s_i) x_{ij}^k \quad \forall k \in K, i, j \in V_c \tag{27}$$

$$q_i^p \geq 0 \quad \forall i \in V_c, p \in P \tag{28}$$

$$\sum_{k\in K}\sum_{h\in b.} y_{ip}^{kh} = 1 \quad \forall i \in V_c, p \in P \tag{29}$$

$$\sum_{i\in S}\sum_{j\in S} x_{ij}^k \leq |S| - 1 \quad S \subseteq V, S \neq \emptyset, \forall k \in K \tag{30}$$

$$x_{ij}^k (1 - x_{ij}^k) = 0 \quad \forall i \in V, j \in V, k \in K \tag{31}$$

$$y_{ip}^{kh}(1-y_{ip}^{kh})=0 \quad \forall i \in V, p \in P, h \in h_k, k \in K \tag{32}$$

Among these, Equation (21) represents the objective of minimizing total costs, including vehicle fixed costs, transportation costs, refrigeration costs, carbon emission costs, and time window penalty costs; Equation (22) represents vehicles departing from the distribution center, serving customers, and ultimately returning to the distribution center; Equation (23) represents that when a vehicle passes through arc $e(i, j)$, customer j accepts the delivery service; Equation (24) represents the balance of vehicle traffic when visiting customers; Equation (25) represents that the delivery demand for any product by each customer does not exceed the corresponding delivery vehicle's cargo capacity; Equation (26) represents that a single service should aim to deliver as many cold chain products as possible; Equation (27) represents the time relationship between the preceding and succeeding nodes when the vehicle arrives at customer j; Equation (28) represents that customer demand is non-negative: Equation (29) indicates that customer demand is indivisible; Equation (30) indicates the elimination of subloops: Equations (31) and (32) are decision variables. Equation (31) indicates that if vehicle k travels from customer i to customer j, it is 1; otherwise, it is 0. Equation (32) indicates that if vehicle k's cargo compartment h satisfies customer i's demand for product type p, it is 1; otherwise, it is 0.

4 Optimization of carbon emission reduction pathways for green supply chain logistics

4.1 Improving the NSGA-II Model Solution

4.1.1 Chromosome Encoding and Population Initialization

Based on the typical characteristics of the inventory distribution optimization problem presented in this paper, an encoding design was developed using an improved NSGA-II heuristic algorithm. A real number encoding consisting of two chromosome strings was designed to represent the solution to the problem, as shown in Figure 4.

Central warehouse floor	1	1	1	1	1	1	1	1	1	1	1	1	1	1
Front warehouse layer	2	2	2	2	2	2	2	3	3	3	3	3	3	3
Retail store floor	7	8	9	10	11	12	13	14	15	16	17	18	19	20

First distribution layer	1	2	3	1	2	4	5	1	3	2	1	3	4	1	5	2
Second distribution layer	2	8	12	10	14	0	3	18	15	16	19	20	0	4	22	23

Figure 4: Chromosome coding scheme

The first part of the chromosome consists of three layers of fixed-length chromosomes. The three layers of chromosomes correspond to the retail store layer, the front-end warehouse layer, and the central warehouse layer, respectively. Among them, the central warehouse layer has only one gene position, which stores the corresponding position. The gene values of each gene position in the front-end warehouse layer are the node numbers of the front-end warehouse, while the gene values of each gene position in the retail store layer are the node numbers of the retail stores, the allocation relationship between the retail stores and the front-end warehouses, and the delivery volume for each cycle.

The second part consists of two non-fixed-length chromosomes. The first layer is used to represent the delivery path from the central warehouse to the front warehouse, with gene positions consisting of the central warehouse P and the front warehouse S. Vehicles depart from and return to the central warehouse, and the central warehouse gene position is used to initiate a new path. The second layer represents the delivery path from the front warehouse to the retail store, with gene positions consisting of the front warehouse set S, the retail store set Z, and the virtual 0 set N_{dummy}. Vehicles depart from and return to the front warehouse, with the front warehouse gene position used to initiate a new delivery path. This part of the encoding depends on the allocation relationship of the chromosomes in the first part.

The construction of the initial solution affects the quality of the final solution and the efficiency of the solution process, as randomly generating the initial population impacts the overall evolutionary search efficiency of the algorithm. To improve the evolutionary search process, this paper uses ls to enhance the initial population.

4.1.2 Non-dominant ordering and crowding value calculation

The non-domination ordering in NSGA-II first requires the establishment of dominance relationships. In single-objective problem solving, each individual has only one value, and different individuals can be compared based on this value. Let the values of two individuals be a and b, respectively. There are three possible cases: $a > b$, $a < b$, and $a = b$. In multi-objective problems, individuals are interconnected and influence each other, so the simple comparison of values used in single-objective problems is no longer applicable. Multi-objective problems typically use dominance as a measure, with the following criteria:

Assume there are n objective components $f_i(x), i = 1, 2, \ldots, n$; for any two given individuals p and q, with respect to the n objectives, if the value of p is not worse than that of q for each objective, and p has at least one objective value that is better than q, then p is said to be better than q, p is dominant or in a non-dominated position, and q is dominated, denoted as: $p > q$.

To ensure population diversity, NSGA-II allows further selection within each non-dominated level of the same ranking order. Therefore, it uses crowding degree as an indicator to measure and determine the density around an individual. In this method, the non-dominated level of an individual is first obtained; the lower the non-dominated level, the relatively better the individual. Within the same non-dominated level, the crowding distance of each individual is calculated to obtain a partial order set for further selection. The relatively more advantageous individuals have larger crowding distances.

4.1.3 Cross-operation

NSGA-II selects a solution from the population for crossover operation, which directly acts on the second part of the chromosome. The crossover process is as follows:

Step 1: Select two individuals from the current population with probability p_c as parent chromosomes $P1$ and $P2$.

Step 2: Randomly select two crossover gene positions $cp1$ and $cp2$ from the chromosomes, and swap the middle parts of the $cp1$ and $cp2$ gene positions between $P1$ and $P2$

Step 3: Finally, conflict detection is performed. The exchanged gene pairs are mapped to each other, and the duplicate genes in the exchanged individuals are converted through mapping. This operation is repeated until there are no conflicts in the individuals. At this point, the crossed offspring $O1$ and $O2$ are obtained.

4.1.4 Variation Operations

This paper proposes a random mutation operation based on gene positions, where the mutation operation directly acts on the second part of the chromosome. A chromosome $P3$ is randomly selected as the parent chromosome with probability p_m. First, the subpath with the fewest targets is randomly deleted from the parent chromosome. Then, the deleted customers are reinserted into other subpaths using the insertion method, while ensuring that all constraints are satisfied. The specific steps are shown in Figure 5. The subpath 2-6-9 with the fewest customers is deleted from chromosome $P3$, resulting in a new chromosome after deletion. Then, the customer nodes 6 and 9 are reinserted using the insertion method, yielding the offspring $O3$.

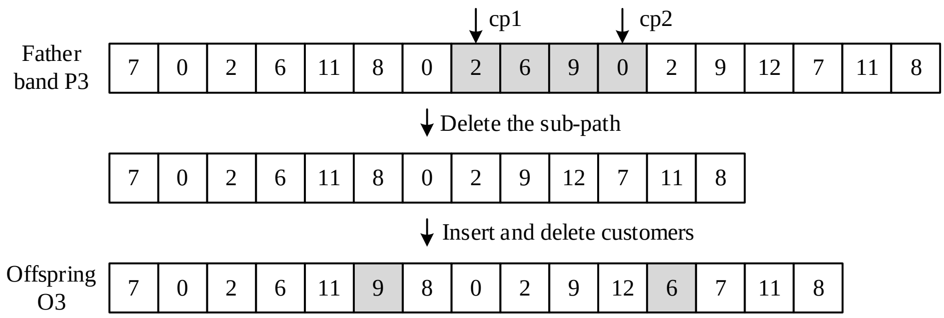

Figure 5: Schematic diagram of mutation operation

4.1.5 Elite retention strategy

The Elite Selection Strategy involves selecting N (population size) outstanding individuals from the merged population of parents and offspring within the same generation to form the parent population for the next generation. The Elite Selection Strategy prevents the loss of Pareto optimal solutions by retaining the superior individuals from the parent generation and directly incorporating them into the offspring generation. Both the parent and offspring populations have a size of N. After merging, a population of size 2N is obtained. Subsequently, a fast non-dominated sorting and crowding distance calculation are performed, and the top N individuals are selected to form the new population. The specific steps are as follows:

Step 1: Merge the parent population and offspring population into a single population.

Step 2: Based on the Pareto ranking of this population from highest to lowest, sequentially place all individuals in this tier into the new parent population until a Pareto tier cannot be fully accommodated.

Step 3: For each Pareto level, calculate the crowding degree of the individuals and add them to the new parent population in order of crowding degree until the new parent population is filled, at which point the new population is obtained.

4.1.6 Domain Search Structure

LS is a classic optimization algorithm that searches multiple “local regions” to find local optima. The neighborhood structure defines how new solutions are generated through local evolution, so the design of a scientific and effective neighborhood structure is a core element in implementing LS.

4.2 Numerical experiments

4.2.1 Parameter Settings

Construct a numerical experiment example with a distribution center and 30 customer points. The distribution center has three different types of refrigerated trucks: A (small), B (medium), and C (large). The location, demand, and service time window of each customer are known, as shown in Table 5. The relevant parameters of each type of refrigerated truck are shown in Table 6.

Table 5: Customer information

Serial number	X-axis	Y-axis	Demand (t)	$[e_i, l_i]$	$[E_i, L_i]$	t_{si} (min)
0	22	42	0.1	5:30-17:00	5:30-17:30	0
1	40	48	1.8	6:00-8:00	5:30-9:00	22
2	37	19	0.8	7:30-9:00	7:00-9:30	12
3	57	47	1.8	6:00-8:00	6:00-8:00	22
4	23	68	1.0	7:30-9:30	7:00-10:30	17
5	18	33	2.2	6:40-8:30	6:10-10:00	27
6	33	28	0.8	7:30-9:30	7:00-10:30	12
7	23	53	1.8	7:20-9:00	7:00-9:30	24
8	14	46	1.0	7:30-9:00	7:00-10:00	17
9	57	62	1.0	7:00-8:30	6:40-9:30	17
10	32	92	1.0	7:00-9:00	6:30-9:40	17
11	57	22	1.8	6:30-8:20	6:00-9:00	22
12	54	39	0.8	7:30-9:00	7:00-10:00	12
13	28	33	2.2	7:00-9:00	6:30-10:20	27
14	16	11	1.8	7:30-9:00	7:00-10:00	22
15	32	7	2.2	6:50-8:30	6:20-9:30	27
16	15	25	1.8	7:00-8:40	6:40-9:30	22
17	10	35	1.8	7:00-8:40	6:40-9:30	22
18	37	37	0.8	7:50-9:00	7:00-10:00	12
19	17	62	2.8	6:30-8:30	6:00-9:30	32
20	47	67	1.0	7:50-9:00	7:70-10:10	17
21	24	24	1.8	7:00-9:00	6:30-9:30	22
22	47	22	1.0	6:30-8:10	6:00-8:40	17
23	13	63	0.8	7:30-9:00	7:00-10:00	27
24	27	17	1.0	7:10-8:50	6:40-9:30	12
25	52	12	2.2	7:00-8:40	6:30-9:30	24
26	55	60	1.8	6:40-8:30	6:00-9:20	18
27	17	52	1.0	7:30-9:30	7:00-10:30	12
28	33	53	0.8	7:20-9:00	6:50-9:40	36
29	41	11	2.8	7:40-9:10	7:00-10:00	17
30	27	72	1.0	6:50-8:40	6:20-9:40	22

Table 6: Refrigerated vehicle parameters

Optimized path	Q^m (ton)	f^m (yuan/unit)	c_{ij}^{mk} (yuan/km)	c_r^m (yuan/hour)	$c_r^{m'}$ (yuan/hour)	ρ_0^m (liter/km)	ρ_*^m (liter/km)
1	6	185	2.6	11	15	0.141	0.291
2	8	215	2.8	13	18	0.155	0.332
3	10	245	4	16	22	0.167	0.343

The algorithm parameters designed in this chapter are as follows: population size is 110, crossover probability P_{c1} = 0.8, P_{c2} = 0.7, mutation probability P_{m1} = 0.1, P_{m2} = 0.01, and maximum iteration count is 400. The algorithm program for solving the model was written in Matlab R2021a. The computer hardware configuration includes an Intel(R) Core(TM) i7-7700HQ CPU, 8 GB of memory, and the Windows 10 operating system.

4.2.2 Analysis of Results

To investigate whether using a carbon emission reduction path optimization model in the cold chain distribution of agricultural products always results in lower total costs compared to single-vehicle distribution, this section sets different customer scales: small-scale (1–10 customer points), medium-scale (1–20 customer points), and large-scale (1–30 customer points). We calculate and compare the various costs of using mixed-path delivery and individual-path delivery under the constraint of achieving an average customer satisfaction rate of 80% for each customer scale. The carbon emission reduction paths used in delivery with the carbon emission reduction path optimization model for different customer scales are shown in Figure 6.

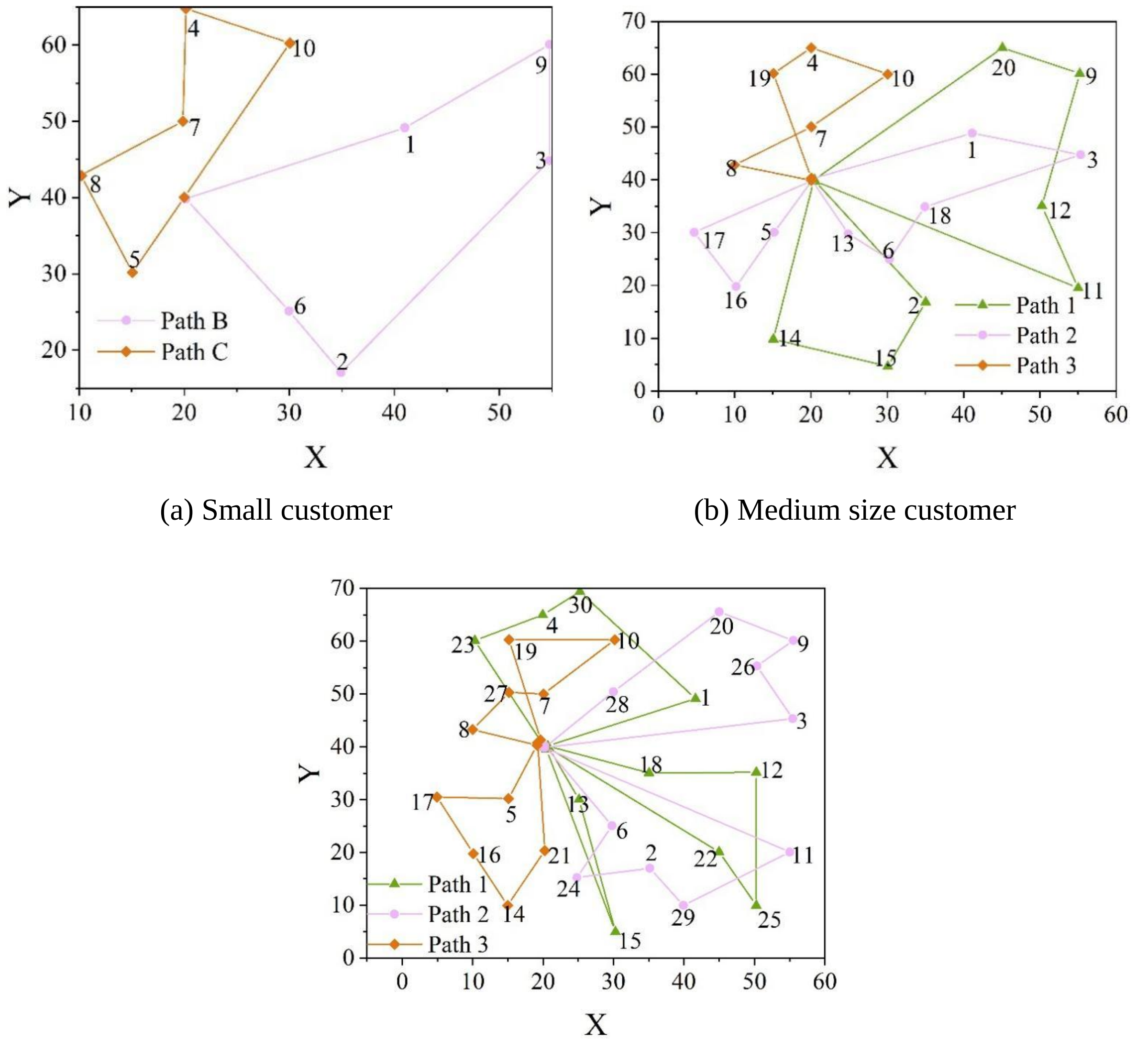

(a) Small customer

(b) Medium size customer

(c) Mass customer

Figure 6: Different scale customer path distribution roadmap

The cost data for different transportation methods under various customer scales are shown in Table 7. As shown in the table, under the carbon emission reduction path optimization model delivery method, the total cost is not always lower than that of single-vehicle delivery across different customer scales. For small and medium-sized customer groups with fewer customers, the total cost of single-vehicle delivery is lower than that of the carbon emission reduction path. As the number of customers increases, the advantages of the carbon emission reduction path optimization model delivery method become increasingly evident, with costs significantly lower than those of single-vehicle delivery. In the large-scale case study, the carbon emission reduction path optimization model reduces total costs by 19.25% compared to Path 1 single-vehicle delivery, by 9.75% compared to Path 2 single-vehicle delivery, and by 7.80% compared to Path 3 single-vehicle delivery. Therefore, when green supply chain management faces delivery tasks for large-scale customers, the carbon emission reduction path optimization model transportation delivery scheme proposed in this paper can be selected.

Table 7: The cost of various distribution modes of different sizes

Delivery path	Number of vehicles	Fixed cost	Transport cost	Damage cost	Refrigerating cost	Time penalty cost	Carbon cost	Assembly book	Actual satisfaction
Small customer									
Optimized path	455	565.318	38.61	100.28	66.98	125.92	1346.19	565.318	83.57%
1	545	538.258	16.08	85.99	114.37	123.42	1417.2	538.258	83.89%
2	425	540.828	59.16	91.49	51.03	135.05	1296.64	540.828	88.74%
3	485	615.948	63.35	118.4	87.82	138.81	1503.41	615.948	82.94%
Medium size customer									
Optimized path	7	1127	1099.53	69.39	190.78	162.44	273.11	2794.85	83.93%
1	9	1280	1214.09	22.12	182.86	188.52	293.62	3140.81	83.95%
2	7	1060	1086.24	53.92	190.68	150.36	259.77	2770.57	86.57%
3	6	980	1237.29	130.6	236.79	145.09	280.92	2970.29	83.49%
Mass customer									
Optimized path	9	1540	1598.68	90.57	276.3	119.75	401.28	3899.94	88.54%
1	12	1903	1868.78	29.57	273.68	235.03	474.55	4654.97	79.77%
2	10	1709	1693.45	114.39	288.85	221.29	412.81	4174.15	79.08%
3	8	1450	1711.18	131.5	322.27	179.34	381.3	4138.95	85.81%

5 Conclusion

In the study of predictive models for carbon emissions in green logistics, ARIMA predictive models were constructed separately for carbon emissions from transportation processes, transshipment processes, and refrigeration processes. A case study was conducted for the Beijing-Tianjin-Hebei region, and the results showed that the p-value of the model was $0.535 > 0.05$, with residual values all within twice the standard error. The ARIMA model demonstrated good predictive performance. Subsequently, a carbon emission reduction path optimization model was developed by comprehensively considering fixed costs, transportation costs, refrigeration costs, carbon emission costs, and time penalty costs, and the improved NSGA-II algorithm was employed for solution. Numerical experiment results indicate that when facing different customer scales, using the carbon emission reduction path optimization model for delivery does not always yield cost advantages. In cases with fewer customers, using individual delivery is more cost-effective. As the customer scale expands, the cost advantages of the carbon emission reduction path optimization delivery method become increasingly evident.

About The Author

Hongli Liu, Master, associate professor at Xi'an Traffic Engineering Institute, research interests: Logistics and supply chain management. E-commerce. Email: 17392216060@163.com

Shuyu Sun, Master, work at Xi'an Traffic Engineering Institute, research direction: Supply Chain Management. Email: sunshuyu1990@163.com

References

[1] Mafini, C., & Muposhi, A. (2017). The impact of green supply chain management in small to medium enterprises: Cross-sectional evidence. Journal of Transport and Supply Chain Management, 11(1), 1-11.

[2] Tseng, M. L., Islam, M. S., Karia, N., Fauzi, F. A., & Afrin, S. (2019). A literature review on green supply chain management: Trends and future challenges. Resources, conservation and recycling, 141, 145-162.

[3] Jo, D., & Kwon, C. (2021). Structure of green supply chain management for sustainability of small and medium enterprises. Sustainability, 14(1), 50.

[4] Bu, X., Dang, W. V., Wang, J., & Liu, Q. (2020). Environmental orientation, green supply chain management, and firm performance: empirical evidence from Chinese small and medium-sized enterprises. International journal of environmental research and public health, 17(4), 1199.

[5] Dubey, R., Gunasekaran, A., & Papadopoulos, T. (2017). Green supply chain management: theoretical framework and further research directions. Benchmarking: An International Journal, 24(1), 184-218.

[6] Tumpa, T. J., Ali, S. M., Rahman, M. H., Paul, S. K., Chowdhury, P., & Khan, S. A. R. (2019). Barriers to green supply chain management: An emerging economy context. Journal of cleaner production, 236, 117617.

[7] Balasubramanian, S., & Shukla, V. (2017). Green supply chain management: an empirical investigation on the construction sector. Supply Chain Management: An International Journal, 22(1), 58-81.

[8] Yildiz Çankaya, S., & Sezen, B. (2019). Effects of green supply chain management practices on sustainability performance. Journal of Manufacturing Technology Management, 30(1), 98-121.

[9] Li, J., Anser, M. K., Tabash, M. I., Nassani, A. A., Haffar, M., & Zaman, K. (2023). Technology-and logistics-induced carbon emissions obstructing the Green supply chain management agenda: Evidence from 101 countries. International Journal of Logistics Research and Applications, 26(7), 788-812.

[10] Yu, Z., Golpira, H., & Khan, S. A. R. (2018). The relationship between green supply chain performance, energy demand, economic growth and environmental sustainability: An empirical evidence from developed countries. LogForum, 14(4), 479-494.

[11] Jamali, M. B., & Rasti-Barzoki, M. (2019). A game theoretic approach to investigate the effects of third-party logistics in a sustainable supply chain by reducing delivery time and carbon emissions. Journal of Cleaner Production, 235, 636-652.

[12] Ali, S. S., Kaur, R., Ersöz, F., Altaf, B., Basu, A., & Weber, G. W. (2020). Measuring carbon performance for sustainable green supply chain practices: A developing country scenario. Central European Journal of Operations Research, 28(4), 1389-1416.

[13] Teixeira, C. R. B., Assumpção, A. L., Correa, A. L., Savi, A. F., & Prates, G. A. (2018). The contribution of green logistics and sustainable purchasing for green supply chain management. Independent Journal of Management & Production, 9(3), 1002-1026.

[14] Kaur, R., Patsavellas, J., Haddad, Y., & Salonitis, K. (2022). Carbon accounting management in complex manufacturing supply chains: A structured framework approach. Procedia CIRP, 107, 869-875.

[15] Truant, E., Crocco, E., Corazza, L., & Borlatto, E. (2024). Life cycle thinking and carbon accounting in sustainable supply chains: a structured literature review and research agenda. Sustainability Accounting, Management and Policy Journal.

[16] Zhao, B., Gui, H., Li, H., & Xue, J. (2020). Cold chain logistics path optimization via improved multi-objective ant colony algorithm. Ieee Access, 8, 142977-142995.

[17] Liu, W. (2024). Distribution path optimization of carbon emission-reducing agricultural products in the cold chain from a green economy perspective. Intelligent Systems with Applications, 23, 200413.

[18] Ghosh, P., Jha, A., & Sharma, R. R. K. (2020). Managing carbon footprint for a sustainable supply chain: a systematic literature review. modern supply chain research and applications, 2(3), 123-141.

[19] Noh, J., & Kim, J. S. (2019). Cooperative green supply chain management with greenhouse gas emissions and fuzzy demand. Journal of Cleaner Production, 208, 1421-1435.

[20] Bo Jiao. (2025). Analysis and Prediction of Railway Passenger Flow Patterns Based on the ARIMA Model. Journal of Engineering Innovations & Technology,7(2),25-61.

[21] Weiyi Zhong,Dengshuai Zhai,Wenran Xu,Wenwen Gong,Chao Yan,Yang Zhang & Lianyong Qi. (2024). Accurate and efficient daily carbon emission forecasting based on improved ARIMA. Applied Energy,376(PA),124232-124232.